International Journal of Electrical, Electronic and Communication Sciences
ISSN: 2517-9438
Vol:1, No:3, 2007

A Robust STATCOM Controller for a Multi-Machine Power System Using Particle Swarm Optimization and Loop-Shaping

S.F. Faisal, A.H.M.A. Rahim, J.M. Bakhashwain

***Abstract*—**Design of a fixed parameter robust STATCOM controller for a multi-machine power system through an H-∞ based loop-shaping procedure is presented. The trial and error part of the graphical loop-shaping procedure has been eliminated by embedding a particle swarm optimization (PSO) technique in the design loop. Robust controllers were designed considering the detailed dynamics of the multi-machine system and results were compared with reduced order models. The robust strategy employing loop-shaping and PSO algorithms was observed to provide very good damping profile for a wide range of operation and for various disturbance conditions**.**

***Keywords*—**STATCOM, Robust control, Power system damping, Particle Swarm Optimization, Loop-shaping.

I. INTRODUCTION

THE static synchronous compensator (STATCOM) is a power electronics based synchronous voltage generator that generates a three-phase voltage from a dc capacitor. By controlling the magnitude of the STATCOM voltage the reactive power exchanges between the STATCOM and the transmission line and hence the amount of shunt compensation in the power system can be controlled [1]. In addition to reactive power exchange, a properly controlled STATCOM can also provide damping to a power system [2, 3].

A good number of recent literatures are available on modeling, operation and control fundamentals of the STATCOM [1, 4-5]. While most of the control designs are carried out with linearized models, nonlinear control strategies for STATCOM have also been reported recently [5]. STATCOM controls for stabilization have been attempted through complex Lyapunov procedures for simple power system models [6]. Applications of robust fuzzy logic and neural network based controls have also been reported [7, 8]. The controllers designed on the basis of linear theory are, generally, operating point dependent and hence are not robust in nature. A fixed parameter robust controller designed through graphical loop-shaping procedure was observed to provide good damping characteristics to a single machine power system [9]. However, application of such graphical techniques to multi-machine system is handicapped because of the higher order of the dynamics.

This article presents an H-∞ based fixed parameter robust STATCOM controller design for a multi-machine power system. The realization of the robust controller for the high order multi-machine system through a graphical loop shaping procedure is simplified by embedding a particle swarm optimization (PSO) procedure in the design loop. Simulation results are presented comparing the design by original loop-shaping method as well as PSO based procedure.

Manuscript received June 5, 2007. This work was supported by the electrical engineering department of King Fahd University of Petroleum and Minerals

S.F. Faisal is with the Electrical Engineering Program, The Petroleum Institute, 2533, Abu Dhabi, UAE.(e-mail: sfaisal@pi.ac.ae).

A.H.M.A. Rahim is with the department of Electrical Engineering, K.F. University of Petroleum and Minerals, Dhahran, Saudi Arabia (corresponding author:: P.O. Box# 349, Dhahran 31261, Saudi Arabia; phone: 0096638604986; fax:0096638603535; email:ahrahim@kfupm.edu.sa).

J.M. Bakhashwain is with the department of Electrical Engineering, K.F. University of Petroleum and Minerals, Dhahran, Saudi Arabia.

II. THE SYSTEM MODEL WITH STATCOM

A 4-machine power system with STATCOMs located at the middle of the transmission lines connecting each generator to the rest of the grid is shown in Fig.1. The synchronous generator is represented by a two-axis model for the internal voltages and the swing equations; and its excitation system is assumed to be equipped with IEEE type-ST exciter model. The STATCOM is represented by a first order differential equation relating the STATCOM DC capacitor voltage and current.

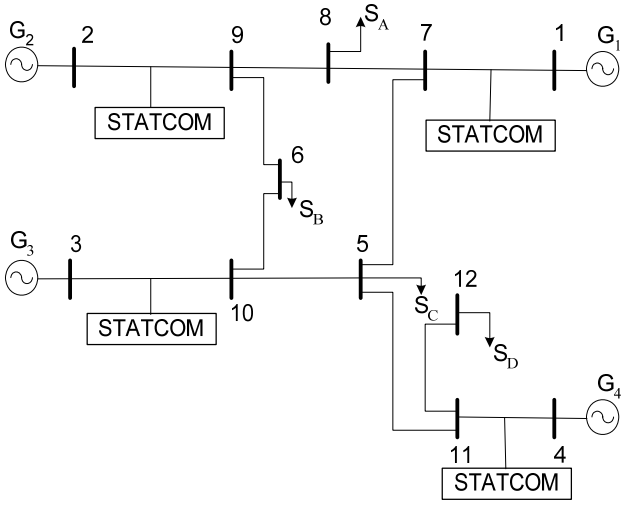

Fig. 1 A 4-machine power system with STATCOM

The dynamic model for the i[th] machine in the power system including its exciter and the STATCOM is expressed in terms of the differential equations given in (1). The circuit configuration of a STATCOM including its location in terms of generator and network buses is shown in Fig.2. A list of the symbols is given in the Nomenclature section.

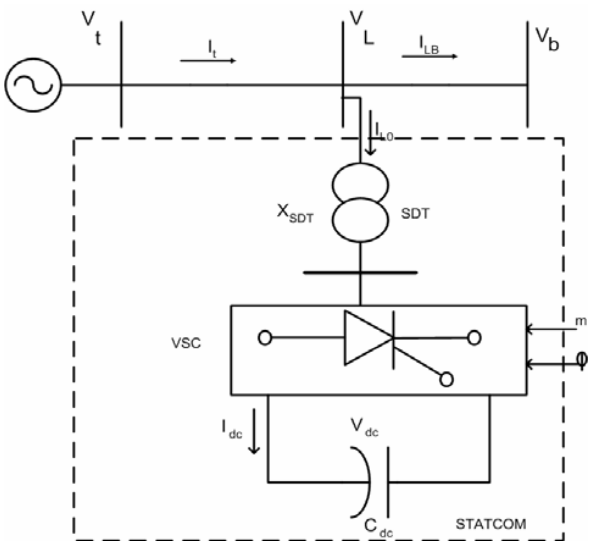

Fig. 2 The STATCOM system representation

$$\dot{e}'_{di} = \left[-e'_{di} + \left(x_{qi} - x'_{di}\right) I_{qi}\right] \frac{1}{T'_{qoi}}$$

$$\dot{e}'_{qi} = \left[E_{fdi} - e'_{qi} - \left(x_{di} - x'_{di}\right) I_{di}\right] \frac{1}{T'_{doi}}$$

$$\dot{\omega}_i = -\frac{1}{2H_i}\left[P_{mi} - P_{ei} - D_i \omega_i\right]$$

$$\dot{\delta}_i = \omega_o \omega_i \qquad (1)$$

$$\dot{E}_{fdi} = -\frac{1}{T_{Ai}} E_{fdi} - \frac{K_{Ai}}{T_{Ai}}\left(V_{toi} - V_{ti}\right)$$

$$\dot{V}_{DCi} = \frac{m_i}{C_{DCi}}\left[I_{sdi} \cos\psi_i + I_{sqi} \sin\psi_i\right]$$

The loads are represented by constant impedances and the load buses are eliminated. The network voltage-current variables are converted to machine d-q frames through the transformation matrix $T_r = \text{diag}[e^{j(\delta-\pi/2)}]$ and the non-state variables in (1) are eliminated. The block diagram in Fig. 3 shows the conversion of the variable from the synchronously rotating network reference frame [D-Q] to individual machine frames [d-q]. The dynamic equations for the multi-machine system are then written as,

$$\dot{x} = f[x,u] \qquad (2)$$

where, the state vector x is composed of variables $[e'_d, e'_q, \omega, \delta, E_{fd}, V_{DC}]^T$ of each machine, and u is the vector of controls [m ψ] of each STATCOM.

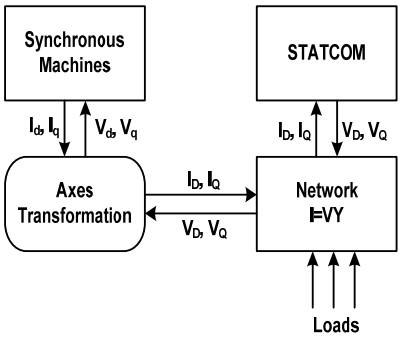

Fig. 3 Diagram showing transformation between the network (D-Q) and machine frames (d-q)

III. Robust Design Using Loop Shaping Technique

The robust control design for the synchronous generator-STATCOM system starts by linearizing the set of equations (2) around a nominal operating point as,

$$\dot{x} = Ax + Bu$$
$$y = Hx \qquad (3)$$

The nominal plant transfer function between the input u and selected output variable y is written as,

$$P = H\,[sI - A]^{-1}\,B \qquad (4)$$

Variations in the plant operating condition is included by a structured uncertainty model as,

$$\tilde{P} = (1 + DW_2)P \qquad (5)$$

W_2 is a fixed stable transfer function, the weight, and D is a variable transfer function satisfying $\|D\|_\infty < 1$. In the multiplicative uncertainty model (5), DW_2 is the normalized plant perturbation away from 1. If $\|D\|_\infty < 1$ then

$$\left|\frac{\tilde{P}(j\omega)}{P(j\omega)} - 1\right| \le |W_2(j\omega)|, \forall \omega \qquad (6)$$

So, $|W_2(j\omega)|$ provides the uncertainty profile and in the frequency plane is the upper boundary of all the normalized plant transfer functions away from 1. For a control function C in cascade with the plant P, the robustness performance and stability measures are satisfied if,

$$\left\| |W_1 S| + |W_2 T| \right\|_\infty < 1 \qquad (7)$$

In the above, W_1 is a real, rational, stable and minimum phase function. T is the input-output transfer function, the complement of the sensitivity function S.

The basic idea of the graphical loop-shaping method is to construct the loop transfer function L = PC to satisfy the robust performance criterion approximately, and then to obtain the controller from the relationship C = L/P. For a monotonically decreasing function W_1, it can be shown that at low frequency the open-loop transfer function L should satisfy,

$$|L| > \frac{|W_1|}{1-|W_2|} \tag{8}$$

while, for high frequency,

$$|L| < \frac{1-|W_1|}{|W_2|} \approx \frac{1}{|W_2|} \tag{9}$$

At high frequency |L| should roll off at least as quickly as |P| does. This ensures properness of C. The general features of open loop transfer function are that the gain at low frequency should be large enough, and |L| should not drop-off too quickly near the crossover frequency to avoid internal instability. Steps in the controller design include: determination of dB-magnitude plots for P and $\widetilde{P}$, finding W_2 from (6), choosing L subject to (7-9), checking for the robustness criteria, constructing C from L/P and checking internal stability. The process is repeated until satisfactory L and C are obtained. The iterative determination of controller C from the choice of open-loop function L, subject to the constraints, are accelerated by incorporating a particle swarm optimization (PSO) technique in the algorithm.

IV. Particle Swarm Optimization

The particle swarm optimization is a population-based optimization tool developed by Eberhart and Kennedy [10]. PSO technique conducts search using a population of particles where each particle is a candidate solution. Particles change their positions by flying around in a multidimensional search space until either computational limits are exceeded or relatively unchanging positions have been encountered. During the flight each particle adjusts its position according to the experience of its own as well as that of the neighboring particle [10-12]. In the PSO algorithm, each particle updates its velocity and position by the relationship,

$$\begin{aligned} V_i(k+1) = Q(k)V_i(k) + K_1\ rand_1[xx]\ \{X_{pbest}(k) - X_i(k)\} \\ + K_2\ rand_2[xx]\ \{X_{gbest} - X_i(k)\} \end{aligned} \tag{10}$$

$$X_i(k+1) = X_i(k) + V_i(k) \tag{11}$$

where, K_1 and K_2 are two positive constants, $rand_1(xx)$ and $rand_2(xx)$ are random numbers in the range [0, 1], and Q is the inertia weight. X_i represents position of the i-th particle and V_i is its velocity. The first term in (10) depends on the former velocity of the particle(s), the second is the cognition modal, which includes particles' own thinking and memory, and the third part represents the socio-psychological adaptation knowledge of the particles. The three parts together determine the space searching ability. The first part has the ability to search for local minimum. The second part causes the swarm to have a strong ability to search for global minimum and avoid local minimum. The third part reflects the information sharing among the particles. Under the influence of the three parts, the particle can reach the best position.

The PSO algorithm starts by initializing the velocity and position of the population of particles randomly. In the first iteration the 'global best' and the 'local best' are set equal. The process is repeated until some acceptable solution is reached or the maximum number of iterations exceeded.

In the proposed PSO based loop-shaping approach the robust controller structure is pre-selected as,

$$C(s) = \frac{b_m s^m + \cdots\cdots + b_1 s + b_o}{a_n s^n + \cdots\cdots + a_1 s + a_o} \tag{12}$$

The open loop function L is then constructed from $L(s) = P(s)C(s)$. The performance index J to be minimized is chosen to include the robustness criteria as well as the constraints on L given by (8-9) and is expressed as,

$$J = \sum_{i=1}^{N} r_i J_{Bi} + r_o J_S \tag{13}$$

where, J_{Bi} are the robust stability indices and J_S is the stability index of the over-all closed loop system. r_i and r_o are the penalties associated with the respective indices and N is the number of frequency points in Bode plot of $L(j\omega)$. At each frequency ω_i, the magnitude of open-loop transmission $L(j\omega_i)$ is calculated and then checked to see whether or not the robust stability bound is satisfied at that frequency. The robust stability indices are defined by,

$$J_{Bi} = \begin{cases} 0, & \text{if bound at } \omega_i \text{ is satisfied} \\ 1, & \text{otherwise} \end{cases} \tag{14}$$

$i = 1,2,3,\ldots\ldots N$

The stability of the closed loop nominal system is tested by solving the roots of characteristic polynomial and then checking whether all the roots lie in the left side of the complex plane. The stability index J_S is defined as,

$$J_S = \begin{cases} 0, & \text{if stable} \\ 1, & \text{otherwise} \end{cases} \tag{15}$$

The coefficients b_m, ...b_1 and a_n, ...,a_1 are searched by the PSO algorithm to minimize J subject to the constraints; a_n being set to 1. The flow chart for the proposed PSO based loop-shaping algorithm is shown in Fig. 4.

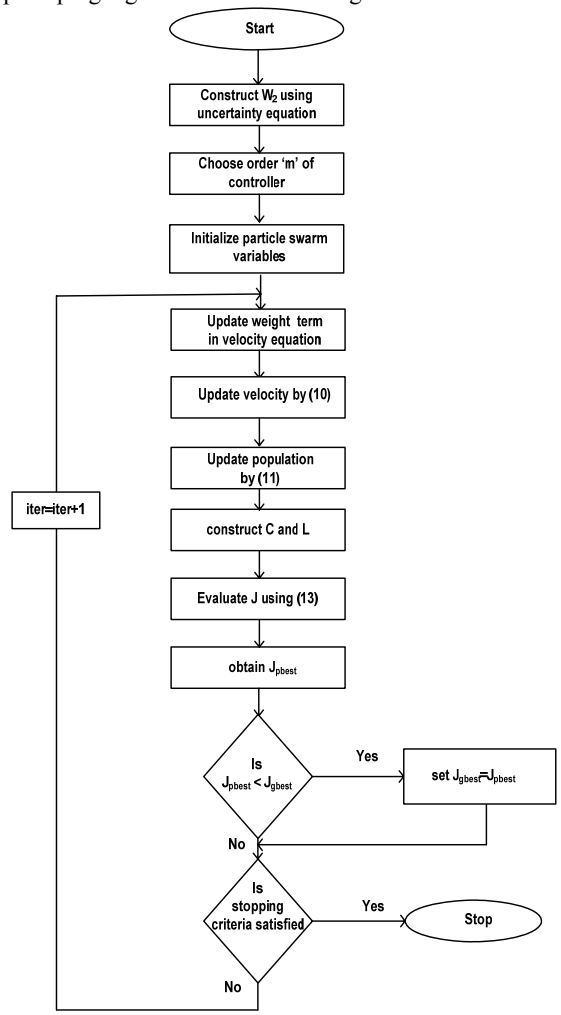

Fig. 4 Flow chart for the proposed PSO based loop-shaping.

V. Robust Design Using Loop Shaping Technique

The robust control design was implemented on the multi-machine power system shown in Fig.1. Considering a STATCOM between generator 2 and bus 9, the detailed dynamic model is expressed in terms of 20 first order equations. A reduced order model was obtained considering the angular speed deviation ($\Delta\omega_2$) of the generator #2 as the plant output and voltage modulation index m of the STATCOM as the input. A balanced realization technique was employed for the reduction procedure [13]. The plant transfer function of the minimum order model which fits that of the detailed model was obtained from several simulation studies. The minimal plant function of the reduced system for the nominal operating point was found to be,

$$P = \frac{-100s(s-40.93)(s+15.27)(s^2+0.66s+17.22)}{s(s+30)(s+4.44)(s+0.33)(s^2+0.62s+31.19)} \quad (16)$$

Off-nominal outputs between 0.4 and 1.4 pu and power factor from 0.8 lagging to 0.8 leading were considered for the different generators. The quantity, $\left|\tilde{P}(j\omega)/P(j\omega)-1\right|$ for each perturbed plant was constructed and the uncertainty profile was fitted to the following function,

$$W_2(s) = \frac{0.191(s+20.6)(s+0.86)}{(s^2+10.01s+25.57)} \quad (17)$$

A Butterworth filter satisfying all the properties for $W_1(s)$ is selected as,

$$W_1(s) = \frac{K_d f_c^2}{s^3+2s^2 f_c+2sf_c^2+f_c^3} \quad (18)$$

For K_d = 0.0001 and f_c = 1, and for a choice of open-loop transfer function L which satisfies the loop-shaping properties outlined in section 3, the relationship L=PC yield the following controller function,

$$C(s) = \frac{16.88(s+2.63)(s+0.71)(s^2+0.63s+0.39)(s^2+0.46s+0.37)}{(s^2+11.41s+79.21)(s^2+1.68s+1.64)(s^2+0.66s+0.67)} \quad (19)$$

VI. The Robust Design With PSO

For the reduced order nominal plant transfer function (16), the PSO starts with W_1 and W_2 arrived at through the loop-shaping procedure of section 5. A second order controller function is selected for the robust design. Following the procedure given in section 4, the PSO algorithm converged to yield the control function,

$$C(s) = \frac{12.82(s+7.33)(s+0.23)}{s^2+3.6768s+77.455} \quad (20)$$

The open-loop function L(s) is then obtained as,

$$L(s) = \frac{-1.281\times10^3 s(s-40.93)(s+15.27)(s+7.33)(s+0.22)(s^2+0.66s+17.22)}{s(s+30)(s+4.44)(s+0.33)(s^2+3.68s+77.46)(s^2+0.62s+31.19)} \quad (21)$$

The parameters used in the PSO algorithm are: $K_1=K_2=2$; maximum and minimum weights for Q are 1.2 and 0.1, respectively. The population size was taken to be 20 and the maximum number of iterations set to 1500.

By considering the 20th order detailed model of the 4-machine power system, the controller function arrived at by the PSO algorithm is,

$$C(s) = \frac{25\times10^3(s+3.9998)(s+0.0002)}{s^2+0.07454s+2.797} \quad (22)$$

Loop shaping plots relating W_1, W_2, and L for reduced order and detailed model with and without PSO are shown in Fig. 5 while, the corresponding performance measures are in Fig. 6. In Fig. 5, the open-loop functions (L) were selected to fit the upper and lower bounds set by (8-9) in all the three cases. With the graphical construction procedure the control structure is more complicated and gave the open-loop function (L) slightly different from those obtained by PSO (b and c). Plot b in Fig. 5 is with the reduced order plant model, while c is with the full-order multi-machine power system model. The plots for the nominal and robust performance measures are shown in Fig. 6. It can be observed that performance measures are almost identical for all the three cases, and that they are well satisfied.

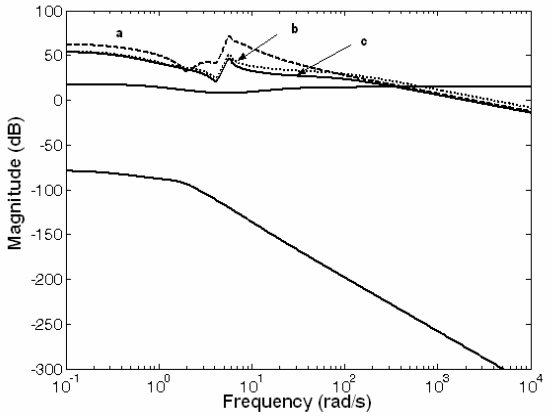

Fig.5 Loop-shaping plots: the open-loop function L for, a) reduced order model through graphical loop-shaping, b) reduced order model through PSO, and c) detailed order model through PSO.

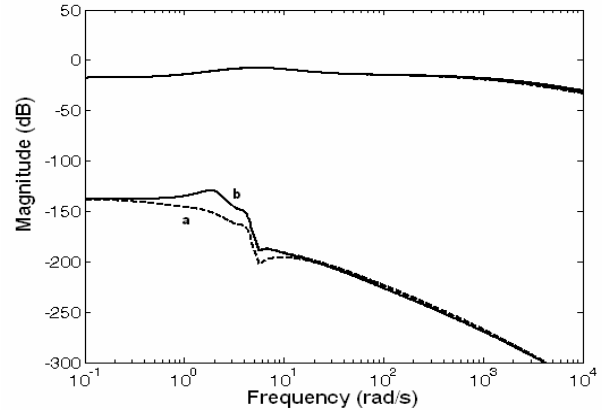

Fig. 6 The nominal and robust performance measures: a) reduced order model through graphical loop-shaping, b) reduced and detailed order models through PSO.

VII. Evaluation Of The Robust Control

The performance of the designed control was evaluated through simulations of the 4-machine power system given in Fig.1. Comparison of the responses with the original graphical loop-shaping control and PSO based loop-shaping methods are given in Figs. 7 and 8. Fig.7 shows the relative rotor angles of the generators for a 50% torque pulse on generator #2 for 0.1 sec at nominal loading with a) no STATCOM control, b) PSO based loop-shaping and, c) original loop-shaping, respectively. The nominal plant function was that of the reduced order model obtained through balance realization. Fig. 8 shows the angle variations when a three phase fault for 0.1 sec is applied at bus 2. The relative rotor angle of the generators are shown for, a) no STATCOM control, b) PSO based loop-shaping and, c) original loop-shaping, respectively. This is a severe disturbance, and in the absence of control action the system is transiently unstable. It can be observed that both the graphical and PSO based loop-shaping techniques produce controller functions that give almost identically good transient control. The reduced order model as obtained through balance realization is employed.

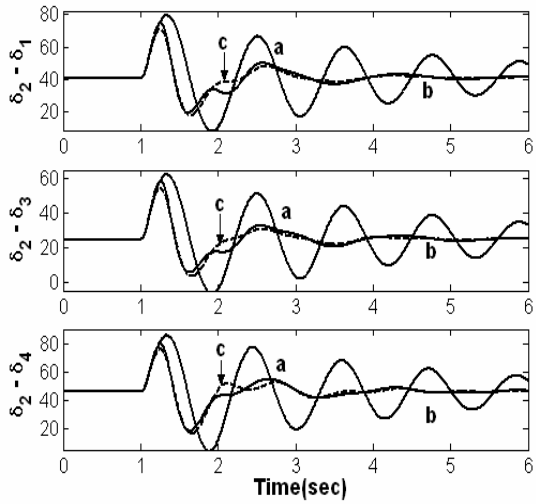

Fig. 7 Comparison of relative angles for a 50% input torque pulse on generator 2 for 0.1s with (a) no control, (b) PSO based loop-shaping, and (c) graphical loop-shaping

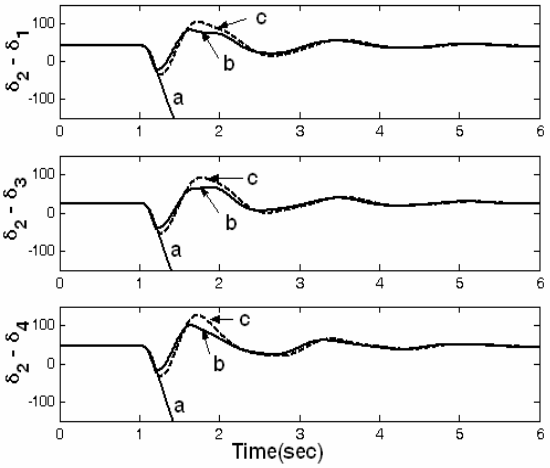

Fig. 8 Relative rotor angles following a 3 phase fault at bus 2 for 0.1 sec with (a) no control, (b) PSO based loop-shaping control, and (c) graphical loop shaping control.

The controller was then tested for a number of other operating conditions. Figs. 9 and 10 show the variation of relative rotor angles for a disturbance of 50% input torque pulse for 0.1 seconds on generator #2 and a three phase fault at bus #2 for 0.1 sec, respectively. The different loading conditions are given in Tables I and II in the Appendix. It can be observed from the figure that the robust controller damps the oscillations very quickly for all these widely different loadings conditions.

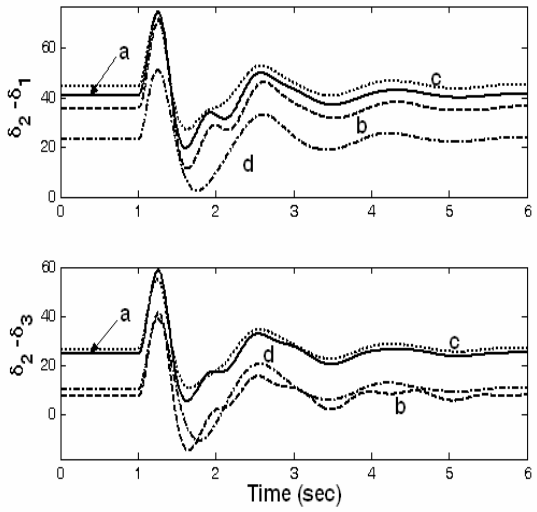

Fig. 9 Relative rotor angle deviations for four different loadings following a 50% torque pulse on shaft of generator #2 for 0.1 sec.

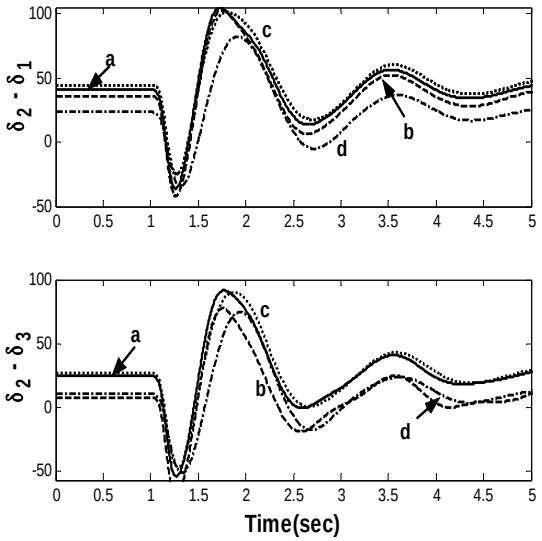

Fig. 10 Relative rotor angle deviations for the loadings of Fig. 9 for a 3 phase fault at bus #2 for 0.1 sec.

VIII. Conclusions

Robust STATCOM controller for a multi-machine power system has been designed through a graphical loop-shaping procedure. Though it's a powerful method, the graphical loop-shaping technique is handicapped by the dimensionality curse. This has been circumvented by embedding a particle swarm optimization procedure in the loop-shaping design. The advantage of using the PSO is that the order of the controller can be chosen a-priori. The validity of the robust design was verified through a reduced order model obtained through a balanced realization technique. The PSO embedded loop-shaping robust STATCOM controller design is computationally efficient and has been observed to provide very good damping profile over a wide range of operation of the multi-machine power system.

Nomenclature

δ	Generator rotor angle
ω	Rotor speed
ω_o	Base (synchronous) speed
P_m	Mechanical power input
P_e	Electrical power output
H, D	Inertia constant, damping coefficient of generator
e_q'	Quadrature (q) axis internal voltage
E_{fd}	Field voltage
x_d, x_d'	Synchronous, transient direct (d) axis reactance
I_d	d-component of armature current
K_A, T_A	Exciter gain, time constant
V_t	Generator terminal voltage
E_{fdo}, V_{to}	Nominal field, terminal voltage
V_{dc}	dc capacitor voltage of STATCOM
C_{dc}	Capacitance of dc capacitor
m, ψ	Modulation index, phase of STATCOM voltage

Appendix

TABLE I
GENERATION: P (MW) AND Q (MVAR) FOR VARIOUS TEST CASES

Gen	Case a		Case b		Case c		Case d	
G_1	232	119	307	226	68	19	123	31
G_2	700	244	725	366	535	78	330	49
G_3	300	193	575	336	165	74	165	105
G_4	450	266	675	461	245	111	157	94

TABLE II
LOAD: P (MW) AND Q (MVAR) FOR VARIOUS TEST CASES

Loads	Case a		Case b		Case c		Case d	
S_A	350	195	460	275	275	135	200	150
S_B	350	195	460	275	175	135	125	175
S_C	650	375	900	475	410	250	350	250
S_D	325	155	450	220	150	100	125	75

ACKNOWLEDGEMENT

The authors wish to acknowledge the facilities provided at the King Fahd University of Petroleum and Minerals, Dhahran, Saudi Arabia and the Petroleum Institute, Abu - Dhabi, UAE.

REFERENCES

[1] Noorazi A.H and Sharaf A.M., "Two control schemes to enhance the dynamic ferformance of the STATCOM and SSSC" IEEE Trans. Power Delivery. 2005. Vol. 20 No. 1. PP 435-442.
[2] Rao P, Crow M.L and Young Z., "STATCOM control for power system voltage control applications", IEEE Trans. on Power Delivery. 2000. Vol. 15 No. 4. PP 1311-1317.
[3] Sensarma P.S, Padiyar K.R and Ramnarayanan V., "Analysis and performance evaluation of a distribution STATCOM for compensating voltage fluctuation", IEEE Trans. Power Delivery. 2001. Vol. 16 No. 2. PP259-264.
[4] Ye Y, Kazerani M and Quintana V.H., "Current source converter based STATCOM: modeling and control", IEEE Trans. Power Delivery. 2005. Vol. 20 No 2. PP 795-800.
[5] Soto D and Pena R., "Nonlinear control strategies for cascaded multilevel STATCOM", IEEE Trans. Power Delivery. 2004. Vol.19 No. 4. PP 1919-1927.
[6] Haque M.H and Kumkratng P., "Application of Lyapunov stability criterion to determine the control strategy of a STATCOM", IEEE Proc. – Gener. Transm. Distrib. 2004. Vol.151 No. 3. PP 415-420.
[7] Mak L.O, Ni Y.X and Shen C. M., "STATCOM with fuzzy controllers for interconnected power systems", Electric Power Systems Research. 2000. Vol. 55. PP 87-95.
[8] Mohaddes M, Gole A.M and McLaren P.G., "A neural network controlled optimal pulse-width modulated STATCOM", IEEE Trans. Power Delivery. 1999. Vol.14 No. 2. PP 481-488.
[9] Rahim A.H.M.A and Kandlawala F.M., "Robust STATCOM voltage controller design using loop-shaping technique", Electric Power System Research. 2004. Vol. 68. PP 61-74.
[10] Kennedy J and Eberhart R., "Particle swarm optimization", 1 IEEE International Conference on Neural Networks. 1995. Vol. 4. PP 1942-1948.
[11] Yuhui S.R and Eberhart R., "Empirical study of PSO", IEEE, Proceedings of the 1999 Congress on Evolutionary Computation. 1999. Vol. 3. PP 6-9.
[12] Kennedy J., "The particle swarm optimization social adaptation of knowledge", International Conference of Evolutionary Computation. 1997. PP 303-308.
[13] Sam R, Postlethwaite I and Gu D., "Model reduction with balanced realizations", International Journal of Control. 1995. Vol. 62. PP 33-64.

S.F. Faisal was born in Hyderabad, India in 1978. He received his B.Tech Electrical Engineering degree from JNT University; Hyderabad, India in 2001and M.Sc. from the K.F.University of Petroleum and Minearls (KFUPM) in 2005. He is working as Lab Engineer in the Electrical Engineering Program of The Petroleum Institute, Abu-Dhabi, UAE since Sep. 2006. His major area of interest is power system analysis, FACTS devices & control, artificial intelligence and optimization.

Abu H. M.A.Rahim (S'69, M'72, SM'83) did his B.Sc. in Electrical Engineering from the Bangladesh University of Engineering and Technology (BUET), Dhaka in 1966 and Ph.D. from the University of Alberta, Edmonton, Canada in 1972. After a brief post-doctoral work at the University of Alberta, he rejoined the Faculty in BUET, Dhaka. Dr. Rahim was a Visiting Fellow at the University of Strathclyde, Glasgow (U.K.) in 1978. Since then he worked at the University of Bahrain, University of Calgary and at the K.F.University of Petroleum and Minerals, where he is now a Professor. Dr. Rahim's main fields of interest are Power System Stability, Control and Optimization. Dr. Rahim is a Fellow of the Institute of Engineers, Bangladesh.

Jamil M. Bakhashwain, is an Associate Professor and Chairman of Electrical Engineering Department at King Fahd University of Petroleum & Minerals, Dhahran, Saudi Arabia. He received his Ph.D. from University of Colorado at Boulder in 1989. His areas of interests are control systems and its application and measurements and management of magnetic fields on transmission lines. He has published many journal and conference papers and authored or co-authored a number of technical reports. He has been involved in many research projects and studies on power system.